FRANCIELE BRAGA MACHADO TULLIO
LUCIO MAURO BRAGA MACHADO
(ORGANIZADORES)

AMPLIAÇÃO E APROFUNDAMENTO DE CONHECIMENTOS NAS ÁREAS DAS ENGENHARIAS

Atena
Editora
Ano 2020

FRANCIELE BRAGA MACHADO TULLIO
LUCIO MAURO BRAGA MACHADO
(ORGANIZADORES)

AMPLIAÇÃO E APROFUNDAMENTO DE CONHECIMENTOS NAS ÁREAS DAS ENGENHARIAS

Atena Editora
Ano 2020

2020 *by Atena Editora*
Copyright © Atena Editora
Copyright do Texto © 2020 Os autores
Copyright da Edição © 2020 Atena Editora
Editora Chefe: Profª Drª Antonella Carvalho de Oliveira
Diagramação: Natália Sandrini de Azevedo
Edição de Arte: Lorena Prestes
Revisão: Os Autores

Atena Editora
Ano 2020

Dados Internacionais de Catalogação na Publicação (CIP)
(eDOC BRASIL, Belo Horizonte/MG)

A526 Ampliação e aprofundamento de conhecimentos nas áreas das engenharias [recurso eletrônico] / Organizadores Franciele Braga Machado Tullio, Lucio Mauro Braga Machado. – Ponta Grossa, PR: Atena, 2020.

Formato: PDF
Requisitos de sistema: Adobe Acrobat Reader
Modo de acesso: World Wide Web
Inclui bibliografia
ISBN 978-65-86002-74-4
DOI 10.22533/at.ed.744200804

1. Engenharia – Pesquisa – Brasil. 2. Inovações tecnológicas. 3. Tecnologia. I. Tullio, Franciele Braga Machado. II. Machado, Lucio Mauro Braga.

CDD 620

Elaborado por Maurício Amormino Júnior | CRB6/2422

Atena Editora
Ponta Grossa – Paraná - Brasil
www.atenaeditora.com.br

Atena Editora
Ano 2020

APRESENTAÇÃO

Em "Ampliação e Aprofundamento de Conhecimentos nas Áreas das Engenharias" vocês encontrarão dezenove capítulos que demonstram que as fronteiras nas engenharias continuam sendo ampliadas.

A engenharia aeroespacial brasileira vem realizando muitos estudos para a melhoria nos processos de construção de satélites e temos nesta obra quatro capítulos demonstrando isso.

Na engenharia elétrica e na computação temos quatro capítulos demonstrando empenho no aprofundamento de pesquisas envolvendo temas atuais.

A engenharia de materiais e a engenharia química trazem quatro capítulos com pesquisas na produção de novos materiais e produção de medicamentos.

Pesquisas na engenharia de produção temos três capítulos que demonstram o empenho na análise de qualidade da produção industrial.

Os demais capítulos apresentam boas pesquisas em engenharia civil, engenharia mecânica e engenharia agrícola.

Boa leitura!

Franciele Braga Machado Tullio
Lucio Mauro Braga Machado

SUMÁRIO

CAPÍTULO 19

CONSTRUÇÃO, INSTRUMENTAÇÃO E CARACTERIZAÇÃO DE UM TÚNEL DE VENTO DIDÁTICO DE CIRCUITO FECHADO

Data de aceite: 27/03/2020

Data de submissão: 03/01/2020

Lucas Ramos e Silva
Departamento de Engenharia Mecânica (DEMEC) – Escola de Engenharia – Universidade Federal de Minas Gerais (UFMG)
Belo Horizonte – Minas Gerais
http://lattes.cnpq.br/0128562534314022

Guilherme de Souza Papini
Departamento de Engenharia Mecânica (DEMEC) – Escola de Engenharia – Universidade Federal de Minas Gerais (UFMG)
Belo Horizonte – Minas Gerais
http://lattes.cnpq.br/8484713679248812

Rafael Alves Boutros
Departamento de Engenharia Mecânica (DEMEC) – Escola de Engenharia – Universidade Federal de Minas Gerais (UFMG)
Belo Horizonte – Minas Gerais
http://lattes.cnpq.br/5330774619018840

Romero Moreira Silva
Departamento de Engenharia Mecânica (DEMEC) – Escola de Engenharia – Universidade Federal de Minas Gerais (UFMG)
Belo Horizonte – Minas Gerais
http://lattes.cnpq.br/1831447718635688

Wender Gonçalves dos Santos
Departamento de Engenharia Mecânica (DEMEC) – Escola de Engenharia – Universidade Federal de Minas Gerais (UFMG)
Belo Horizonte – Minas Gerais
http://lattes.cnpq.br/0210149443584373

RESUMO: O presente estudo tem como objetivo descrever a construção e a caracterização inicial de um túnel de vento de circuito fechado em escala reduzida, visando estudos de dinâmica de fluidos experimental e teórica para estudantes de graduação e pós-graduação. As atividades ocorreram no Laboratório de Aerodinâmica Experimental, pertencente ao Departamento de Engenharia Mecânica da Universidade Federal de Minas Gerais, em Belo Horizonte / MG, Brasil. Este modelo é um túnel de vento atmosférico de baixa velocidade em circuito fechado, que está sendo usado para calibrar modelos teóricos e desenvolver conhecimentos sobre o tratamento de turbulência. Foi produzido em placas de acrílico de 0.010 m de espessura, flangeadas com placas de alumínio de 0.003 m de espessura. A seção em que o motor fica e a região imediatamente a montante da seção de teste foram construídas com ácido polilático (PLA) pelo processo de Fabricação Aditiva (impressão 3D). Testes experimentais foram realizados para determinar a eficiência do difusor e a perda de pressão na seção de teste

do túnel de vento, a fim de iniciar o processo de caracterização.
PALAVRAS-CHAVE: Túnel de vento, Laboratório, Fabricação, Aerodinâmica Experimental, Didático

CONSTRUCTION, INSTRUMENTATION AND CHARACTERIZATION OF A DIDACTIC CLOSED LOOP WIND TUNNEL

ABSTRACT: The present study aims to describe the construction and the initial characterization of a reduced-scale closed-loop wind tunnel, aiming at both experimental and theoretical fluid dynamics studies for undergraduate and graduate students. The activities took place at the Experimental Aerodynamics Laboratory, which belongs to the Mechanical Engineering Department of the Federal University of Minas Gerais, in Belo Horizonte/MG, Brazil. This model is an atmospheric low-speed closed-loop wind tunnel, which is being used to calibrate theoretical models and develop knowledge about turbulence treatment. It was produced in 0.010 m thickness acrylic plates flanged with 0.003 m thickness aluminum plates. The section in which the motor stands and the region immediately upstream to the test section were built with polylactic acid (PLA) by Additive Manufacturing process (3D printing). Experimental tests were conducted to determine the efficiency of the diffuser and the pressure loss in the wind tunnel test section in order to begin the characterization process.
KEYWORDS: Wind tunnel, Laboratory, Manufacturing, Experimental Aerodynamics, Didactics

1 I INTRODUCTION

Instructions for reduced-sized wind tunnels construction are commonly found in scientific papers, as seen in BHANUPRASAD et al. (2016), due to their great importance in the study of the airflow around an object of interest since they include the full complexity of real fluid flow, according to BARLOW et al. (2007). High costs involved in manufacturing, instrumentation and maintenance, as well as installation complexity due to limitations of physical space, are usually factors associated with large wind tunnels. These factors have allowed smaller-scale wind tunnels to gain ground in undergraduate studies in Mechanical and Aeronautical Engineering, as seen in CALAUTIT et al. (2014) and PELT et al. (2010).

This document intends to present the process of manufacturing a closed-loop small-scale wind tunnel, as well as to demonstrate that small scale models can generate experiments that can be applied in practical classes of Experimental Aerodynamics, generating knowledge to assist in addressing real engineering problems. As such, this present work presents the main steps of manufacturing a wind tunnel in 1:10 scale of an existing closed-loop wind tunnel available in the Experimental Aerodynamics Laboratory at the Federal University of Minas Gerais (UFMG) main campus. This equipment is the result of a voluntary undergraduate research project approved by the Department of Mechanical Engineering at UFMG, which includes the Aerospace Engineering bachelor's degree.

As an undergraduate research project, the conducted research also intended to develop the authors' skills in investigating, applying theoretical knowledge and solving a real engineering application that demanded project planning, equipment scaling, budget estimation, construction and testing. Finally, the results obtained in this work show that this reduced-scale wind tunnel can be used to perform experiments and research aimed at obtaining knowledge in the area of fluid dynamics applied to aerodynamics.

2 I METHODOLOGY

2.1 Design and construction

As the study was based on the closed-loop wind tunnel located in the Experimental Aerodynamics Laboratory of the UFMG Aerospace Engineering bachelor's degree, the research project began with the measurement of each part of the tunnel in actual size. Thus, with all measurements taken, the wind tunnel was divided into 9 different sections, numbered according to Figure 1, to facilitate manufacturing and handling. The nomenclature of each section is presented on Table 1.

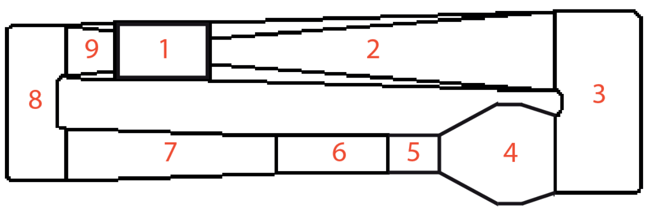

Figure 1 - Wind tunnel sections. By the authors.

Section number	Nomenclature
1	Motor Section
2	Tertiary Diffuser
3	Flow Redirector at Propeller Downstream
4	Nozzle at Test Section Upstream
5	Elongation
6	Testing Section
7	Primary Diffuser
8	Flow Redirector at Propeller Upstream
9	Secondary Diffuser

Table 1 - Nomenclature of the wind tunnel sections. By the authors.

The sizes of each of these sub-parts were reduced by a 1:10 scale factor in order to perform the laser cutting of the acrylic plates that compose the major part of the structure. Sections 1 and 5 were manufactured using a 3D printing process from polylactic acid (PLA), the first one responsible for housing the motor and the propeller that moves the mass of air in the wind tunnel. The reason for the production of these two parts through a 3D printing process was its low cost and practicality, since the laboratory has partnered with other additive manufacturing laboratories. Also, the printing was achieved with optimum precision of the printed parts, facilitating the fixing of the commercial motor to the hub of the manufactured propeller, ensuring a tight assembly between the propulsion cell and the ducts that compose the wind tunnel. Details regarding the choice of the motor and the propeller will be discussed later in this paper.

The following figures illustrate the dimensions of the other wind tunnel sections in millimeters after the scaling process. Also, a brief description of the role of each section is presented.

Section 1 has its initial and final internal cross-section dimensions accordingly to the octagonal geometry of the sections 9 and 2, respectively illustrated in Figures 9 and 2. Using CAD software, a loft operation was made to gradually change this format to a circular one at the center cross-section of this part, where the propeller is located. The diameter of this central circular section is 0.165 m. The result obtained is presented in Figure 12 in text section 2.1.3. This part is not present on the original large scale equipment. However, because of the reduced size of the scale model, the manufacturing of this piece was necessary to provide support for the chosen electric motor and propeller. Figure 2 to 9 shows the dimensions for the sections 2 till 9.

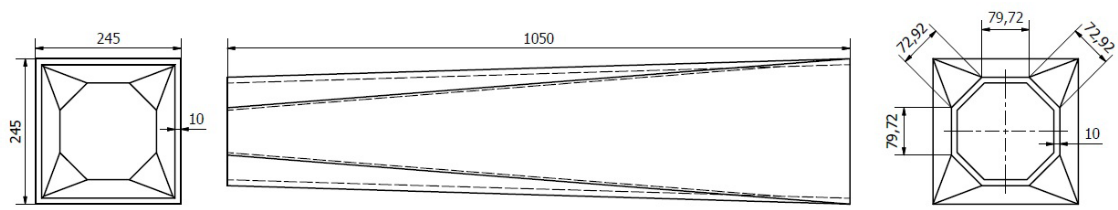

Figure 2 - Tertiary Diffuser (Section 2).

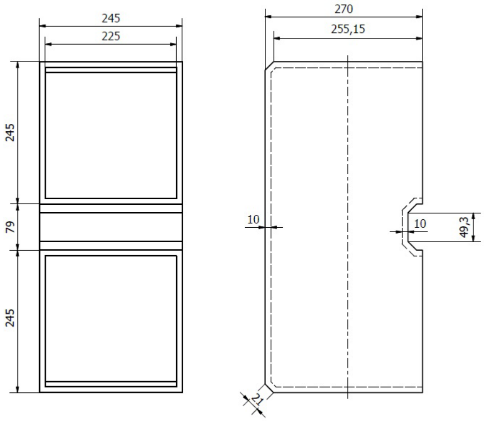

Figure 3 - Flow Redirector at Propeller Downstream (Section 3). Dimensions in millimeters. By the authors.

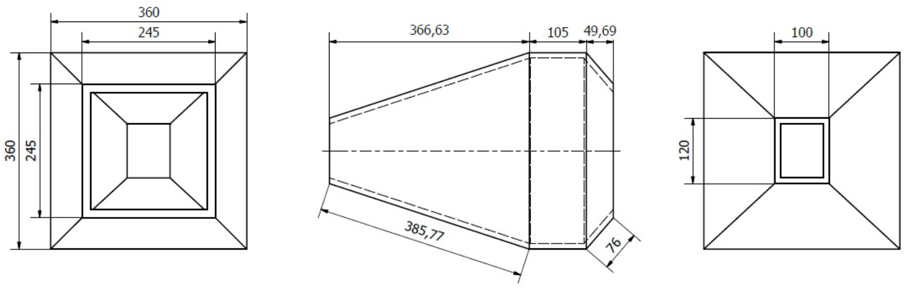

Figure 4 - Nozzle at Test Section Upstream (Section 4). Dimensions in millimeters. By the authors.

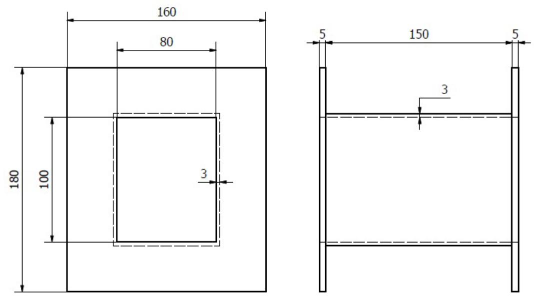

Figure 5 - Elongation (Section 5). Dimensions in millimeters. By the authors.

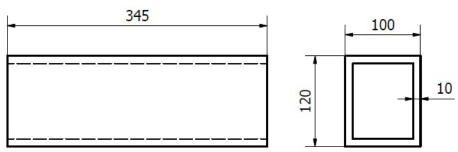

Figure 6 - Testing Section (Section 6). Dimensions in millimeters. By the authors.

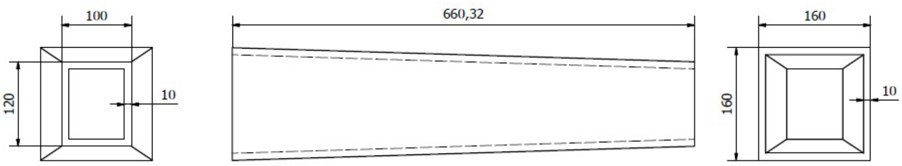

Figure 7 - Primary Diffuser (Section 7). Dimensions in millimeters. By the authors.

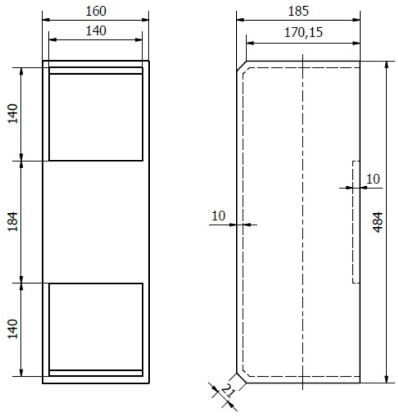

Figure 8 - Flow Redirector at Propeller Upstream (Section 8). Dimensions in millimeters. By the authors.

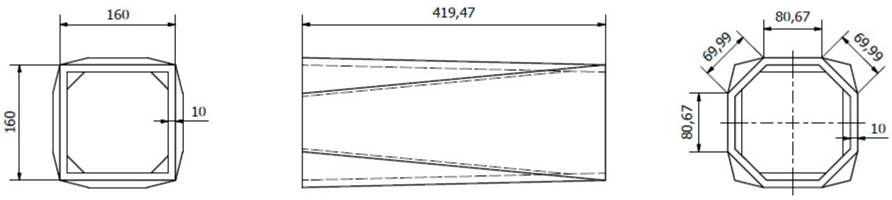

Figure 9 - Secondary Diffuser (Section 9). Dimensions in millimeters. By the authors.

2.1.1 Acrylic components

The choice of using acrylic plates in most of the tunnel structure is due to its fine surface finish, adequate mechanical strength and also its translucent appearance that meets the didactic purpose of visualizing the internal components of a closed-loop wind tunnel.

After obtaining the acrylic pieces already cut accordingly to the pre-established dimensions and joining the plates that form each one of the sections together with epoxy glue, as seen on Figure 10, the corners of each section were smoothed out using polyester resin.

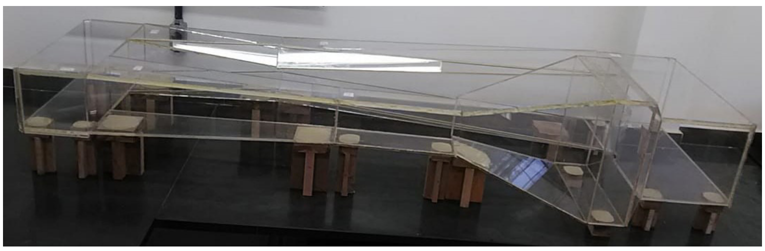

Figure 10 - The acrylic pieces glued with epoxy. By the authors.

In Figure 11, the aluminum flanges were glued to the external faces of the acrylic walls using silicone and the sections of the closed circuit wind tunnel were connected to each other by screws, washers and bolts attached to these flanges.

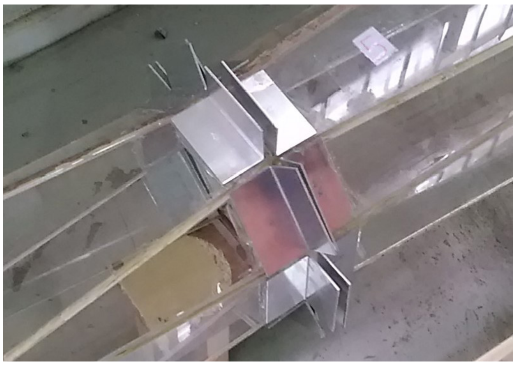

Figure 11 - The aluminum flanges. By the authors.

2.1.2 Printed Components

PLA is a commonly used polymer in additive manufacturing due to its relatively high mechanical resistance and easy handling. In the present work, the 3D printer extruder and bed temperatures chosen are, respectively, 463 K and 333 K. There are four different types of printed components (or group of components) in the wind tunnel: propeller, propeller section, propeller support and elongation section. The first three ones compose the section 1 and the last one is the section 5.

2.1.3 Propeller and motor

The propeller used to move the air along the wind tunnel is designed based on the method for optimum propeller design found in the article by ADKINS AND LIEBECK (1994).

As proposed in the work by TORRES (2018), the propeller designed consists of seven blades and it is optimized for an advance ratio of 1.35. The external propeller diameter is restricted to 0.160 m due to compatibility with the adjacent acrylic sections. Its hub has a diameter of 0.035 m and it is designed to internally accommodate the electric brushless motor responsible for its rotation, as shown in Figure 12. In order to increase its mechanical strength and avoid geometric imperfections, the propeller was printed with 100% infill.

The motor used to spin the propeller is a 2300 KV brushless DC motor model EMAX 2205 designed for racing drones. The motor shaft has a M5 thread which allows it to be attached to the propeller by a nut.

Based on the propeller's advance ratio, the wind tunnel's propeller-motor system was designed to move the air at 18 m while running in a rotational speed of 5000 revolutions per minute. That airspeed in the propeller section would represent in the test section an average wind speed of about 48 m, regarding only the cross sectional area ratio (2.67) of those parts.

Figure 12 - Propeller and its section. By the authors.

2.1.4 Propeller Section

The propeller section intends to smoothly change the octagonal section geometry of the acrylic structure into a circular one, then change it back into an octagonal one in the flow perspective. Additionally, it holds the propeller support inside the wind tunnel. This section consists of two jointed parts attached by four M5 bolts. Both parts are composed of four printed pieces attached by PVC adhesive (this division is required due to the limited size of the 3D printer bed). The fact that the section is not structurally critical allows the application of 30% infill in printing. Section geometry was built to match the real acrylic sections geometry.

2.1.5 Propeller support

The propeller support attaches the motor-propeller system by four M3 bolts and keeps its position inside the propeller section. It also protects and accommodates the electric motor wires from the airflow. It is printed with 70% infill because of its structural function and it is attached by PVC adhesive to one of the propeller section parts.

2.1.6 Elongation Support

The elongation section intends to correct the final geometry of the wind tunnel, close the circuit and match the acrylic made test section and nozzle geometries adequately. Due to the same reason discussed in section 2.1.4, the elongation section components were printed with 30% infill.

2.1.7 Brushless motor control and power source

The electric motor used in the project is a model commonly employed in RC airplanes. To control the rotation of this device, a commercial electronic speed control unit (ESC) was used. The ESC unit receives the control signal from an Arduino microcontroller that has a 10 k potentiometer connected to it. A 30 A power supply was used to provide the required direct current to the motor.

2.2 Instrumentation

In order to characterize the wind tunnel properties, as well as to obtain flow control data during the tests, several holes were drilled along the sections for the installation of static pressure taps. A hole for a Pitot tube was also drilled in the test section of the equipment.

The static outlets were made by installing aluminum tubes with an outside diameter of 0.001 m in holes made with that same drill diameter. Each tube was initially fixed in place using cyanoacrylate adhesive and the attachment surroundings were then sealed with silicone. Figure 13 shows a close view of all the static taps installed on the top of the test section of the tunnel.

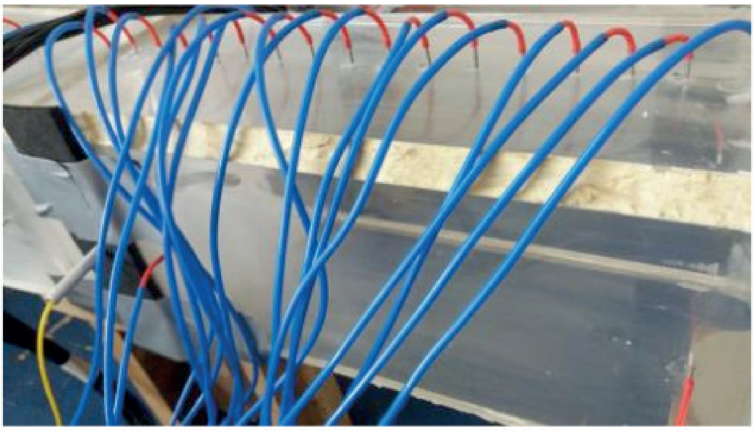

Figure 13 - Static pressure taps on the test section. By the authors.

The Pitot tube was made with an aluminum tube of 0.006 m external diameter, folded at 90°, with another inner tube of 0.001 m diameter fastened to the tip of the larger tube using an epoxy adhesive. The inner tube was connected to a flexible hose, responsible for communicating with the measuring instrument, and then attached in alignment with the center of the outer tube. The schematic design of the construction and the final results are shown in Figure 14. It is worth noting that the choice for the pressure-taking pipes diameters was made to match the connection with the measurement equipment available in the laboratory.

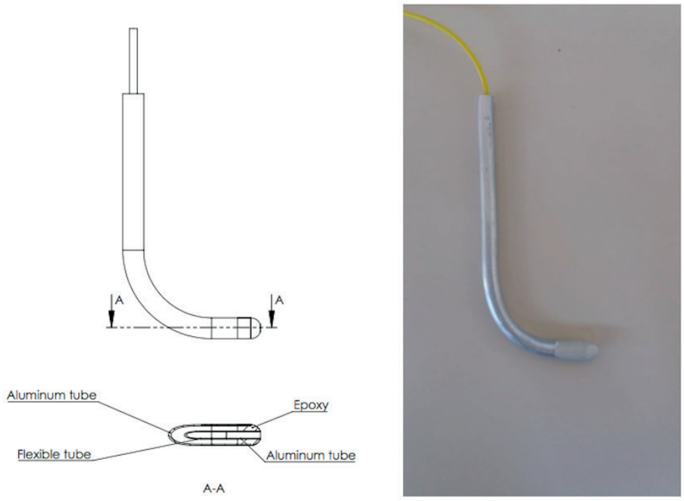

Figure 14 - Pitot tube. By the authors.

2.3 Characterization

In order to validate that the reduced-sized wind tunnel is able to fulfill its main purposes, some experiments were conducted. Those experiments can be found in EASTLAKE (2007), used in regular Experimental Aerodynamics classes at Embry-Riddle Aeronautical University. The first test determines the diffuser efficiency, whereas the second one investigates the longitudinal static pressure distribution. The tests are described in the next subsections.

2.3.1 Diffuser Efficiency Test

Diffusers are used in wind tunnels to increase the static pressure by reducing the flow velocity, converting dynamic into static pressure. Hence, the Diffuser Efficiency is directly related to the reduction of the tunnel power required to reach a specified test section velocity.

The increase in static pressure between the inlet and the outlet of the diffuser, or the static pressure recovery, is a commonly used performance parameter, as stated in EASTLAKE (2007).

For this test, alongside the reduced-sized wind tunnel, a digital manometer and a Pitot-static system in the high speed section are necessary.

The tunnel must be run in two different throttle settings. The static and total pressure in the test section shall be measured, alongside the static pressure within 3 different locations on the diffuser wall. Unsteadiness in the static pressure reading must be verified as this may be a sign of surging. The pressure recovery coefficient is given by Equation 1, in which and are the static and dynamic pressure, respectively, in the subscript location.

$$C_{pr} = \frac{P_{s,outlet} - P_{s,inlet}}{q_{inlet}} \quad (1)$$

The ideal pressure recovery coefficient $C_{pr.ideal}$ is given by Equation 2.

$$C_{pr,ideal} = 1 - \left(\frac{A_{inlet}}{A_{outlet}}\right)^2 \quad (2)$$

In the equation above, means the cross-sectional area in the subscript location. Finnaly, the efficiency n_p is given by Equation 3.

$$\eta_p = \frac{C_{pr}}{C_{pr,ideal}} \quad (3)$$

That efficiency is expected to be between 0.70 and 0.75 for a reasonably good diffuser.

2.3.2 Longitudinal static pressure distribution test

This experiment is used to determine how the free stream static pressure varies from the upstream end to the downstream end of the test section. That longitudinal static pressure distribution is important as it enables the verification of whether the boundary layer thickness increases as the flow moves downstream, which decreases the effective cross-sectional area and requires the use of a correctional factor for any drag data measured in the test section.

According to EASTLAKE (2007), the representation of the longitudinal static pressure gradient magnitude is done by using a non-dimensional factor k developed by GLAUERT (1923), which is expressed in Equation 4.

$$k = -\frac{dP_s}{dl}\frac{B}{q_0} \quad (4)$$

In the equation above, P_s is given in Pascal, l is the test section length in meters, B is the test section width in meters and q_0 is the test section dynamic pressure in Pascal. The derivative $\frac{dP_s}{dl}$ is calculated using a linear fit to the data measured along the test section.

Alongside the reduced-sized wind tunnel, this experiment also requires a manometer and a row of several static pressure taps above the test section with minimum spacing between them.

The tunnel must be run in a typical test speed. The static pressures for each tap are taken, a graph displaying the difference between P_s and the atmospheric pressure for every tunnel station is plotted and the Glauert factor calculated. For a well designed wind tunnel test section, should be between 0.016 and 0.04, according to EASTLAKE (2007).

3 I RESULTS

The construction represents an important achievement by this paper and Figure 15 shows the result achieved in this step.

Figure 15 - The wind tunnel built for the project. By the authors.

It is important to mention that all the tests were performed in lower wind velocities than initially planned. The motor employed for the experiments showed limitations in operating with the designed fan. The main problem faced was the overheating of the brushless motor in a small operation time. This indicates that the provided torque is not enough to overcome the static pressure inside the tunnel, which prevents the achievement of higher wind velocities. For future work, the use of a different electric motor or a new propeller design is recommended. These solutions have not been implemented yet by the authors due to budget constraints.

The diffuser efficiency test was performed in section 7 of the wind tunnel. The three pressure measurements were taken at $l_{dif\ fuser} = 0.06$ m, $l_{dif\ fuser} = 0.32$ m, and $l_{dif\ fuser} = 0.59$ m, where $l_{dif\ fuser}$ represents the distance from the beginning of the diffuser segment, as demonstrated in Figure 16. From now on, these sections will be referenced by the subscripts 1,2 and 3, respectively, and the subscript 1,2 refers to the value computed between 1 and 2. The values obtained from three distinct static pressure taps were averaged to calculate the static pressure in each region of the diffuser. The total pressure was obtained at the end of the test section, that is the segment 6 of the tunnel. The dynamic pressure was computed by the subtraction of the static value from the total pressure, both measured at the same location on the test section. The wind velocity used in the experiment is $V_{ts} = 4.55$ min the the test section. The results for the pressure recovery between each diffuser cross-section are presented in Table 2.

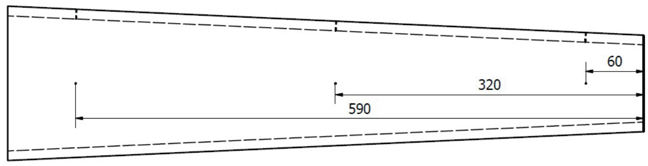

Figure 16 - Diffuser pressure taps positioning. By the authors.

$C_{pr_{1,2}}$	$C_{pr_{2,3}}$	$C_{pr_{1,3}}$
0.2827	0.3062	0.5889

Table 2 - Pressure recovery coefficient C_{pr}. By the authors.

Table 3 shows the values for the ideal pressure recovery and Table 4 the efficiency of each sector.

$C_{pr_{ideal_{1,2}}}$	$C_{pr_{ideal_{2,3}}}$	$C_{pr_{ideal_{1,3}}}$
0.4756	0.4524	0.7128

Table 3 - Ideal Pressure recovery coefficient $C_{pr\ ideal}$. By the authors.

$\eta_{p_{1,2}}$	$\eta_{p_{2,3}}$	$\eta_{p_{1,3}}$
0.5944	0.6768	0.8261

Table 4 - Diffuser Efficiency n_p. By the authors.

Comparing the results obtained between sections 1 and 3 of the diffuser, presented in the last column of Table 4, with the literature reference mentioned in text section 2.3.1, the obtained value is higher than 75%, which is an indicative of great pressure recovery efficiency.

For the longitudinal static pressure distribution test, a total of 17 taps, 0.0165 m apart from each other, were installed at the top of the test section. However, problems encountered during data acquisition demonstrated that the last one was not installed correctly and its results were discarded. Figures 17 and 18 show the manometric pressure measured at each of the remaining points, at two different velocities.

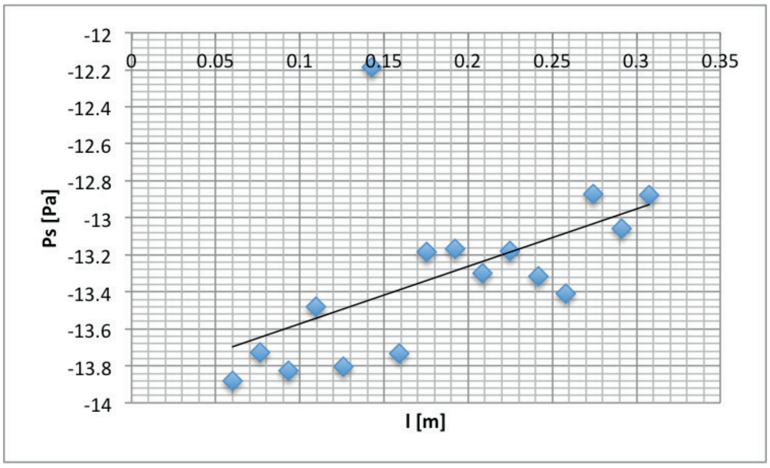

Figure 17 - Static pressure distribution on the test section at V_{ts} = 4.45 m. By the authors.

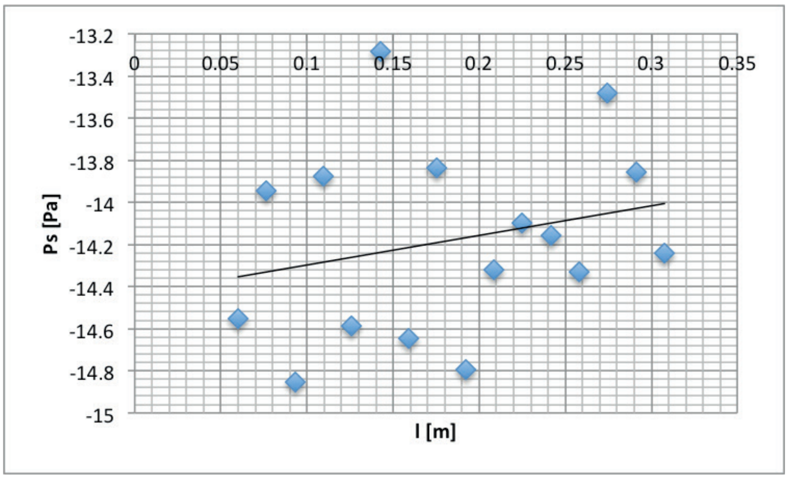

Figure 18 - Static pressure distribution on the test section atV_{ts} = 4.55 m. By the authors.

As the trendlines in Figures 17 and 18 illustrate, the values obtained are well dispersed, especially for V_{ts} = 4.55 m.$^{s-1}$. Both inclinations are positive, demonstrating that the static pressure rises along the test section instead of dropping as expected. Table 5 contains the values calculated for the Glauert's non-dimensional factor k, for each velocity, and the data used for it. The test section width considered was 0.1 m.

V_{ts} $[\mathrm{m} \cdot \mathrm{s}^{-1}]$	q_0 [Pa]	$\frac{dP_s}{dl}$	k
4.45	10.661	3.102	-0.029
4.55	11.113	1.406	-0.013

Table 5 - Glauert factor . By the authors.

As demonstrated, the results show a great dispersion, increasing with the increment on the velocity. It happens because the tunnel stream is not treated, and it may indicate great turbulence in the test section. Also, Pitot tubes usually are not precise on velocities below 10 m.$^{s-1}$ Another factor to consider is the Pitot tube positioning inside the section that may have caused an excessive airflow perturbation and consequently the data dispersion. The reduced tunnel dimensions make it very sensitive to the effects caused on the flow by objects located inside it. The hole used for the total pressure tap installation provides an opening for the atmosphere and that can also increase the static pressure. Tests performed at higher wind velocities may show better results as the tunnel runs closer to its intended conditions.

4 I CONCLUSIONS

The diffuser test presented an efficiency value of 82.61% when the entire section is considered. That value is above 75%, which is the literature reference. However, the results for the longitudinal pressure distribution in the test section indicate that the wind tunnel requires a great amount of work to improve the stream characteristics. The future activities performed on the equipment, aiming the flow treatment, are key to promote students' knowledge, consequently enabling the formation of new professionals trained to perform wind tunnel tests.

The tunnel was built and tested as described. It currently is part of the Experimental Aerodynamics Laboratory of Federal University of Minas Gerais and is undergoing new tests and improvements to enhance its usage range and reliability. Even though the tests showed that a great pressure recovery efficiency was found, some geometry and motor torque issues still affect the overall performance of the tunnel and extra improvements and further studies should be conducted.

ACKNOWLEDGMENTS

This work was first presented at the II Congresso Aeroespacial Brasileiro (II CAB) and the authors would like to thank the conference organizing committee.

REFERENCES

ADKINS, C.N.; LIEBECK, R.H. **Design of optimum propellers**. Journal of Propulsion and Power, v. 10, n. 5, p. 676–682, 1994.

BARLOW, J.B.; POPE, A; RAE, W.H. **Low-Speed Wind Tunnel Testing.** 3rd ed. Chichester, New York: Wiley, 2007.

BHANUPRASAD, D.; MURTHY, S.; SRINIVA, G.; APPALARAJU, G. **Design and fabrication of wind tunnel.** International Journal & Magazine of Engineering, Technology, Management and Research, v. 3, n. 6, p. 271–277, 2016.

CALAUTIT, J.K.; CHAUDHRY, H.N.; HUGHES, B.R.; SIM, L.F. **A validated design methodology for a closed-loop subsonic wind tunnel.** Journal of Wind Engineering and Industrial Aerodynamics, v.

125, p. 180–194, 2014.

EASTLAKE, C.N. **Experimental Aerodynamics and Wind Tunnels.** 7th ed. Daytona Beach: Embry-Riddle Aeronautical University, 2007.

GLAUERT, H. **The interference of wind channel walls on the aerodynamic characteristics of an aerofoil**. Reports and memoranda, n. 867, Aeronautical Research Committee, 1923.

PELT, R.V.; ZOBECK, T.; BADDOCK, M.; COX, J. **Design, construction and calibration of a portable boundary layer wind tunnel for field use.** American Society of Agricultural and Biological Engineers. Transactions, v. 53, n. 5, p. 1413–1422, 2010.

TORRES, G.M.; **Projeto de hélices contrarrotativas**. Belo Horizonte: Universidade Federal de Minas Gerais, Bachelor's Thesis, 2018.

SOBRE OS ORGANIZADORES

FRANCIELE BRAGA MACHADO TULLIO Engenheira Civil (Universidade Estadual de Ponta Grossa - UEPG/2006), Especialista em Engenharia de Segurança do Trabalho (Universidade Tecnológica Federal do Paraná – UTFPR/2009, Mestre em Ensino de Ciências e Tecnologia (Universidade Tecnológica federal do Paraná – UTFPR/2016). Trabalha como Engenheira Civil na administração pública, atuando na fiscalização e orçamento de obras públicas. Atua também como Perita Judicial em perícias de engenharia. E-mail para contato: francielebmachado@gmail.com

LUCIO MAURO BRAGA MACHADO Bacharel em Informática (Universidade Estadual de Ponta Grossa – UEPG/1995), Licenciado em Matemática para a Educação Básica (Faculdade Educacional da Lapa – FAEL/2017), Especialista em Desenvolvimento de Aplicações utilizando Tecnologias de Orientação a Objetos (Universidade Tecnológica Federal do Paraná – UTFPR/ 2008). É coordenador do Curso Técnico em Informática no Colégio Sant'Ana de Ponta Grossa/PR onde atua também como professor desde 1992, também é professor na Faculdade Sant'Ana atuando nas áreas de Metodologia Científica, Metodologia da Pesquisa e Fundamentos da Pesquisa Científica e atua como coordenador dos Sistemas de Informação e do Núcleo de Trabalho de Conclusão de Curso da instituição. E-mail para contato: machado.lucio@gmail.com

ÍNDICE REMISSIVO

A

B

C

D

E

F

T

Atena
Editora
2020